

Fine-structure splitting of exciton states in quantum dot molecules: symmetry and tunnel-coupling effects

Dong Xu, Nan Zhao, and Jia-Lin Zhu*

Department of Physics, Tsinghua University, Beijing 100084, People's Republic of China

(Dated: November 18, 2018)

Exciton levels and fine-structure splitting in laterally-coupled quantum dot molecules are studied. The electron and hole tunneling energies as well as the direct Coulomb interaction are essential for the exciton levels. It is found that fine-structure splittings of the two-lowest exciton levels are contributed from the intra- and interdot exchange interactions which are greatly influenced by the symmetry and tunnel-coupling between the two dots. As the inter-dot separation is reduced, fine-structure splitting of the exciton ground state is largely increased while those of the excited states are decreased. Moreover, the dependence of the fine-structure splitting in quantum dot molecules on the Coulomb correlation is clearly clarified.

PACS numbers: 71.35.-y, 78.67.-n, 71.70.Gm, 78.55.Cr

I. INTRODUCTION

During the last few years, there are intensive studies on the optical properties of single semiconductor quantum dots (QDs), since they exhibit atom-like energy spectrum and sharp lines in photoluminescence as well as the advantage that they can be conveniently manipulated by the external fields. Semiconductor QDs have been demonstrated as one of the candidates for the single-photon or entangled two-photon sources, which make them very attractive for applications in the fields of quantum cryptography and quantum teleportation.^{1,2,3,4,5,6,7} In the first proposal for a QD-based source of polarization entangled photon pairs, a necessary condition is that the intermediate monoexciton states for the biexciton radiative decay are energetically degenerate.⁸ However, the III-V self-assembled semiconductor QDs tend to be elongated along the $[110]$ crystal axis and the monoexciton states are split by the anisotropic electron-hole exchange interaction.^{9,10,11,12,13,14} Consequently, much effort is devoted to the reduction of the fine-structure splitting of the intermediate exciton states, e.g., thermal annealing and external field tuning.^{15,16,17,18,19,20,21}

Neglecting the electron-hole exchange interaction, the exciton ground state is four-fold degenerate. For $\text{In}_x\text{Ga}_{1-x}\text{As}$ QDs with C_{2v} or lower symmetry, however, the electron-hole exchange interaction splits the exciton ground state into bright and dark doublets, which are separated by about few hundred μeV .²² Furthermore, the bright doublets are split into two linearly polarized states separated by about tens of μeV .²³ At zero external field, the fine-structure splitting of the bright doublet mainly depends on the anisotropy and size of QDs.^{12,13,14} If a magnetic field is applied in a Voigt configuration, the bright states are mixed with the dark states through the Zeeman term and the dark exciton states become optically active.^{22,23} Due to the Zeeman splitting induced by the magnetic field, the fine-structure splitting of bright doublet could be tuned to zero by the magnetic field.^{6,19} In addition, thermal annealing^{15,16} and an in-plane electric field^{20,21} could lead to a significant reduction of the

fine-structure splitting.

Recently, with the development of high-quality QD structures, it is possible to fabricate either vertically- or laterally-coupled self-assembled QDs, namely “quantum dot molecule” (QDM).^{24,25,26,27,28} The exciton ground states exhibit fine structures induced by the electron and hole tunnel-coupling between the two dots.²⁹ The exciton states and interdot coupling could be manipulated by the electric field in either vertically- or laterally-coupled QDM.^{28,30,31,32,33,34,35} Significant Stark effect^{28,30} and pronounced anticrossing of different excitonic transitions³¹ have been observed in the photoluminescence (PL) spectra. According to several numerical calculations,^{32,35,36} interdot coupling as well as the symmetry between the two dots strongly influence the exciton levels and optical properties.

Previously, we found that fine-structure splitting of the exciton ground state in laterally-coupled QDM could be tuned to zero by applying an in-plane electric field of only few kV/cm, which might overcome the deficiency in a single QD.³⁷ Polarization entangled photon pairs might be prepared in a QDM through the biexciton radiative decay. Thus clarifying the mechanism of the variation of fine-structure splitting in QDMs with various interdot separations is very important. In this paper, we study the symmetry and tunnel-coupling effects on the fine-structure splitting of exciton states in QDMs. Exciton levels of symmetric and nonsymmetric QDMs without the electron-hole exchange interaction are given, and we note that the exciton level spacing is much larger than the electron-hole exchange energies. Fine-structure splittings of the two-lowest exciton levels are contributed from the intra- and interdot exchange interactions. Symmetry and tunnel-coupling in QDM strongly influence the exciton envelope functions, and therefore it is interesting that intra- and interdot exchange interactions might be strongly dependent on the symmetry and tunnel-coupling. Moreover, the variations of the fine-structure splittings of exciton ground and excited states are compared and discussed.

In Sec. II, a microscopic theory of exciton levels and

fine-structure splitting in QDM is formulated. In Sec. III, exciton levels in QDM without the exchange interaction are given and discussed. Fine-structure splittings of few low-lying bright exciton states are shown for both symmetric and nonsymmetric QDMs. The intra- and inter-dot parts of the splittings of the two-lowest exciton levels are given and compared. The effects of the symmetry and tunnel-coupling as well as the Coulomb correlation are clearly clarified. Finally, the results are summarized in Sec. IV.

II. DESCRIPTION OF EXCITON LEVELS AND FINE-STRUCTURE SPLITTING

The exciton fine-structure splitting in the semiconductor QDs is contributed from the electron-hole exchange interaction. The study of the electron-hole exchange interaction requires a clear representation of the spin states of the exciton. In a bulk III-V direct-gap semiconductor, the valence-band edge has Γ_8 symmetry ($J = 3/2$) and the conduction-band edge has Γ_6 symmetry. For the flat InGaAs quantum dots investigated in this paper, the light- ($J_z = \pm 1/2$) and heavy-hole ($J_z = \pm 3/2$) bands are split by several tens of meV due to the strain introduced by the lattice mismatch. Actually, according to an empirical tight-binding calculation,³⁸ the proportion of heavy-hole component in the hole ground state of a flat InGaAs QD is as large as 98.2%. Therefore, it is reasonable that the light-hole and spin-orbit-split $J = 1/2$ valence band could be neglected since we mainly focus on the fine-structure splittings of few low-lying exciton states. The exciton state is composed of four combinations of the valence band and the conduction band, i.e.,

$$|X\rangle = \sum_{m,s} \sum_{r_e, r_h} \psi_{ms}(r_e, r_h) a_{c_s r_e}^\dagger a_{v_m r_h} |0\rangle, \quad (1)$$

where the Wannier function representation of the creation and annihilation operators is used, m and s are the z component of the angular momentum of the heavy-hole valence band and the conduction band, respectively, and $\psi_{ms}(r_e, r_h)$ is the envelope function. The z component of exciton spin for state (m, s) is $s - m$. From the selection rule, the spin ± 1 exciton states might be optically active depending on the orbital envelop functions while the spin ± 2 states are optically inactive, irrespective of the orbital envelop functions. The eigenvalue equation for ψ_{ms} is given as

$$\sum_{m's' r'_e r'_h} [H_1 + V_{\text{ex}}(c_s r_e, v_{m'} r'_h; c_{s'} r'_e, v_m r_h)] \psi_{m's'}(r'_e, r'_h) = E \psi_{ms}(r_e, r_h), \quad (2)$$

with the spin-independent part

$$H_1 = \delta_{r_e r'_e} \delta_{r_h r'_h} \delta_{s' s} \delta_{m' m} \left[\frac{p_e^2}{2m_e} + U_e(r_e) + \frac{p_h^2}{2m_h} + U_h(r_h) - \frac{e^2}{\epsilon|r_e - r_h|} \right], \quad (3)$$

where U_e (U_h) is the confinement potential for the conduction (valence) band electron. The electron-hole exchange interaction V_{ex} can be approximated as

$$\begin{aligned} & V_{\text{ex}}(c_s r_e, v_{m'} r'_h; c_{s'} r'_e, v_m r_h) \\ & \approx \delta_{r_e r_h} \delta_{r'_e r'_h} [\delta_{r_e r'_e} V(c_s r_e, v_{m'} r'_e; c_{s'} r'_e, v_m r_e) \\ & + (1 - \delta_{r_e r'_e}) V(c_s r_e, v_{m'} r'_e; c_{s'} r'_e, v_m r_e)], \end{aligned} \quad (4)$$

The first (second) term of Eq.(4) is the so-called short-range (long-range) exchange interaction. The long-range term can be further approximated through the multipole expansion

$$\begin{aligned} & V(c_s r_e, v_{m'} r'_e; c_{s'} r'_e, v_m r_e) \\ & \approx \vec{\mu}_{c_s, v_m} \frac{[1 - 3\hat{n} \cdot \hat{n}]}{|r_e - r'_e|^3} \vec{\mu}_{v_{m'}, c_{s'}} \end{aligned} \quad (5)$$

with

$$\begin{aligned} n &= \frac{r_e - r'_e}{|r_e - r'_e|} \\ \vec{\mu}_{c_s, v_m} &= e \int d^3 r \phi_{c_s R}^*(r) \vec{r} \phi_{v_m R}(r) \end{aligned} \quad (6)$$

where $\phi_{cs(vm)R}(r)$ is a Wannier function localized at the site R . The matrix element of V_{ex} is given as¹³

$$\begin{aligned} V_{\text{anal}}(ms, m's') & \int d^3 r \psi_{ms}^*(r, r) \psi_{m's'}(r, r) \\ & + \int d^3 r \text{div}_r (\psi_{ms}^*(r, r) \vec{\mu}_{c_s, v_m}) \\ & \times \text{div}_r \left[\int d^3 r' \psi_{m's'}(r', r') \frac{\vec{\mu}_{v_{m'}, c_{s'}}}{|r - r'|} \right] \end{aligned} \quad (7)$$

The analytical part V_{anal} could be written in the matrix form as

$$\begin{aligned} & V_{\text{anal}}(ms, m's') \\ & = (E_X^S - 8\pi/3\mu^2) \begin{pmatrix} 1 & 0 & 0 & 0 \\ 0 & 0 & 0 & 0 \\ 0 & 0 & 0 & 0 \\ 0 & 0 & 0 & 1 \end{pmatrix} \end{aligned} \quad (8)$$

with (m, s) and (m', s') in the order, $(\frac{3}{2}, \frac{1}{2})$, $(\frac{3}{2}, -\frac{1}{2})$, $(-\frac{3}{2}, \frac{1}{2})$, and $(-\frac{3}{2}, -\frac{1}{2})$. The definition of the parameters E_X^S and μ can be found in Ref. 13. The second term of Eq. 7, i.e., the nonanalytic term, has a form given by

$$\begin{pmatrix} * & 0 & 0 & * \\ 0 & 0 & 0 & 0 \\ 0 & 0 & 0 & 0 \\ * & 0 & 0 & * \end{pmatrix} \quad (9)$$

where $*$ indicates nonzero matrix elements. In anisotropic QDs, the nondiagonal elements of Eq. 9 are nonzero, and thus the exciton spin ± 1 states are split into two linearly polarized states. The fine-structure splitting of the doublet is determined by the nondiagonal elements of Eq. 9.

Similar to the assumption in Ref. 12, we use an in-plane anisotropic potential to model a single QD, and the two dots are aligned along the x axis

$$U_{e(h)} = \nu_{e(h)} \left[\theta \left(\frac{b_0}{2} - |y_{e(h)}| \right) \theta \left(\frac{a_0}{2} - |x_{e(h)} + \frac{d+a_0}{2}| \right) + \theta \left(\frac{b_1}{2} - |y_{e(h)}| \right) \theta \left(\frac{a_1}{2} - |x_{e(h)} - \frac{d+a_1}{2}| \right) \right] \quad (10)$$

where the two dots with lateral size a_i and b_i for the i th dot are separated by distance d , and ν_e (ν_h) is the conduction (heavy-hole valence) band offset. The exciton envelope function in QDM can be expanded using the Hermite polynomials as

$$\begin{aligned} \psi(r_e, r_h) = & \sum_{i,j,m,n} C_{ijmn} A_{ijmn} \\ & \times u_i(\alpha x_e) u_j(\alpha y_e) \exp\left[-\frac{1}{2}\alpha^2(x_e^2 + y_e^2)\right] \\ & \times u_m(\alpha x_h) u_n(\alpha y_h) \exp\left[-\frac{1}{2}\alpha^2(x_h^2 + y_h^2)\right] \quad (11) \end{aligned}$$

where $u_i(x)$ is the Hermite polynomial, A_{ijmn} is the normalization coefficient for the Hermite polynomials, C_{ijmn} is the expansion coefficient, and α is a variational parameter. Since we study the flat QDs in this paper, the two-dimensional approximation is assumed in the calculation. About 4800 lowest-energy envelope basis are taken into account in the diagonalization of the spin-independent matrix H_1 to ensure the convergence of the calculation. We note that the matrix elements of the Coulomb interaction could be analytically obtained.³⁹ The fine-structure splitting then could be obtained through the perturbation calculation of the exchange interaction V_{ex} since the exchange energy (tens of μeV) is much less than the exciton level spacing (tens of meV).

III. NUMERICAL CALCULATION AND DISCUSSION

In QDM, the exciton levels are strongly affected by the tunneling of the electron and hole as well as the direct Coulomb interaction. The tunneling energies of the electron and hole in the strong coupling region are much larger than the electron-hole exchange energies. The values of the material parameters used in the calculation are $\nu_h = 81$ meV, $\nu_e = 124$ meV, $m_e = 0.034 m_0$, $m_h = 0.053 m_0$, $\mu = 6 e\text{\AA}$, $\epsilon_r = 14$.

A. Symmetric Quantum Dot Molecule

In Fig. 1, low-lying exciton levels without the electron-hole exchange interaction for two coupled identical dots with $a_0 = a_1 = 16$ nm and $b_0 = b_1 = 20$ nm are shown as functions of the interdot separation d . At larger d (> 8 nm), the coupling between the two dots is very weak and the exciton ground state energy is much close to that

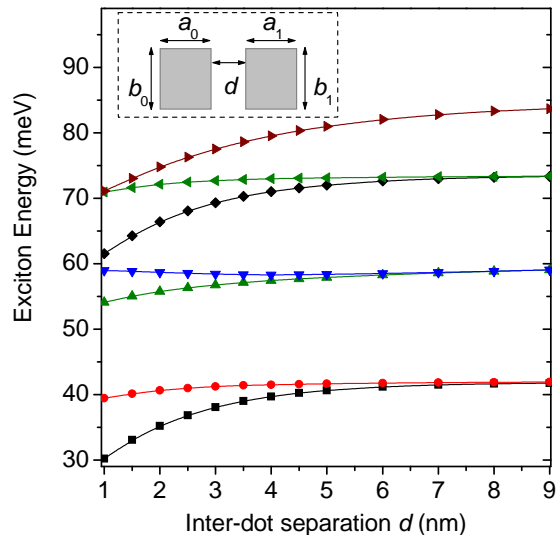


FIG. 1: (Color online) Low-lying exciton levels without the exchange interaction as functions of the interdot separation d for two coupled identical dots with $a_0 = a_1 = 16$ nm and $b_0 = b_1 = 20$ nm. Inset: schematic illustration of a laterally-coupled QDM.

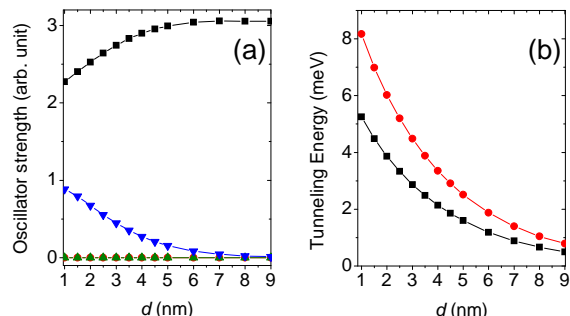


FIG. 2: (Color online) (a) Oscillator strengths of the four lowest exciton states of QDM in Fig. 1 and (b) tunneling energies for the electron (circle) and hole (square), respectively.

of a single isolated dot with $a = 16$ nm and $b = 20$ nm. As the separation d decreases, the interdot coupling is enhanced and the energy levels are split. We note that the four lowest exciton states are mainly composed of the electron and hole ground state in individual dots.³⁶ Their oscillator strengths are shown as functions of d in Fig. 2(a). As d decreases, oscillator strength of the ground state decreases while that of the fourth state increases. The second and third states are always optically inactive, and the fourth state becomes optically inactive as $d > 7.0$ nm. Fig. 2(b) shows the tunneling energies of the electron and hole, which are calculated by the numerical diagonalization of the single particle

Hamiltonian. As d decreases from 9.0 nm to 1.0 nm, the absolute values of the tunneling energies for the electron (hole) increase from 0.79 meV (0.50 meV) to 8.17 meV (5.25 meV).

Exciton levels of QDM without the exchange interaction are each four-fold degenerate and the level spacing is about several meV. If the exchange interaction is included, each of exciton levels is split into fine-structures. One doublet is composed of exciton spin ± 2 states, and the other is composed of exciton spin ± 1 states. For symmetric QDMs in the strong coupling region, the spin ± 1 doublets of the exciton ground and fourth states as shown in Fig. 1 are optically active and could be observed in the PL and PL-Excitation spectra.

In Fig. 3, fine-structure splittings of the exciton ground (δ_1) and fourth (δ_4) states in symmetric QDMs with $a_1 = a_0 = 16$ nm and $b_1 = b_0 = 20$ nm are shown as functions of d . At larger d , the fine-structure splitting δ_1 is negative, e.g., $\delta_1 = -35 \mu\text{eV}$ at $d = 9.0$ nm. As d decreases, δ_1 increases from negative values to positive values. At $d \approx 4.4$ nm, δ_1 is zero. However, δ_4 decreases from zero at larger d to $-150 \mu\text{eV}$ at $d = 1.5$ nm. Although tunnel-coupling induced splitting is negligible at $d = 9.0$ nm as shown in Fig. 1, fine-structure splitting of the exciton ground state is much different from that of the exciton ground state ($-66 \mu\text{eV}$) in a single isolated dot with the same size.

According to Eq. (7), fine-structure splitting of the exciton ground state can be approximated in the first-order as

$$\begin{aligned} \delta_1 &= 2 \sum_{r_e \neq r'_e} \psi_{1,s-m=1}(r_e, r_e) \psi_{1,-1}(r'_e, r'_e) V_{\text{ex}} \\ &= \lambda_{1,\text{intra}} + \lambda_{1,\text{inter}} \end{aligned} \quad (12)$$

with

$$\lambda_{1,\text{inter}} = 2 \sum_{r_e \neq r'_e, x_e x'_e < 0} \psi_{1,1}(r_e, r_e) \psi_{1,-1}(r'_e, r'_e) V_{\text{ex}}, \quad (13)$$

$$\lambda_{1,\text{intra}} = 2 \sum_{r_e \neq r'_e, x_e x'_e > 0} \psi_{1,1}(r_e, r_e) \psi_{1,-1}(r'_e, r'_e) V_{\text{ex}}. \quad (14)$$

where $\psi_{i,s-m}(r_e, r_h)$ is the i th exciton eigenfunction of H_1 with exciton spin z component $s - m$, $\lambda_{1,\text{intra}}$ is indeed the long-range exchange interaction within individual dots, and $\lambda_{1,\text{inter}}$ is that between the two dots (namely the Förster interaction⁴⁰). Fig. 3(b) shows $\lambda_{1,\text{inter}}$ and $\lambda_{1,\text{intra}}$ as functions of d . $\lambda_{1,\text{inter}}$ remains about $20 \mu\text{eV}$ while $\lambda_{1,\text{intra}}$ is greatly changed from $-54 \mu\text{eV}$ at $d = 9.0$ nm to $50 \mu\text{eV}$ at $d = 1.0$ nm.

As discussed in Sec. II, $\psi(r_e, r_h = r_e)$ is directly related to the calculation of the exchange interaction, and therefore it is important for the study of the variation of fine-structure splitting. In Figs. 4(a) and 4(b), $\psi_1(r_e, r_h = r_e)$ and $\psi_4(r_e, r_h = r_e)$ are plotted, respectively. $\psi_1(r_e, r_e)$ is composed of two symmetrically-coupled s state-like functions at larger d . For two dots without the tunnel-coupling,⁴⁰ the Förster interaction (i.e. $\lambda_{1,\text{inter}}/2$) is sim-

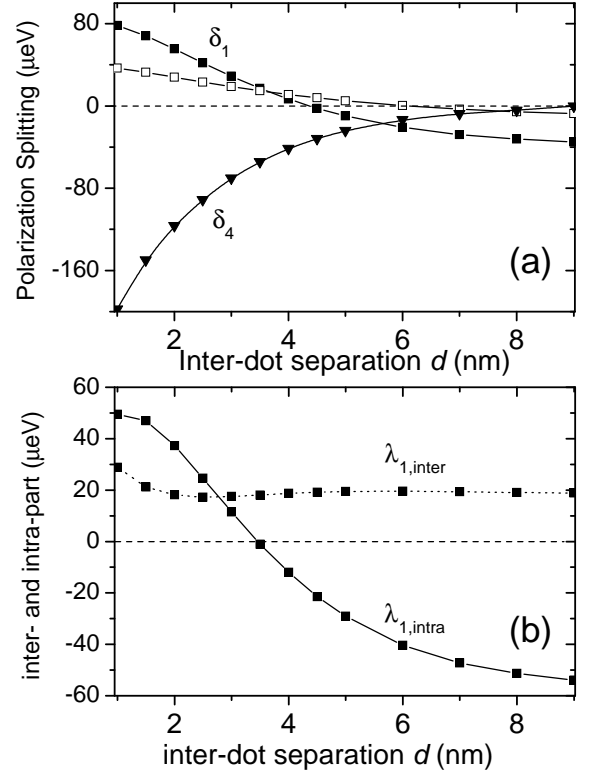


FIG. 3: (a) Fine-structure splitting of the exciton ground state with (square) and without (open square) the Coulomb interaction, and of the fourth exciton state (triangle) of QDM in Fig. 1; (b) $\lambda_{1,\text{intra}}$ and $\lambda_{1,\text{inter}}$ as functions of d .

ply enhanced as d is reduced. However, if the tunnel-coupling can not be neglected as shown in Fig. 4(a), amplitudes of two s state-like functions are reduced at smaller d , which largely compensates the enhancement of $\lambda_{1,\text{inter}}$ at smaller d in the case of neglecting the tunnel-coupling. The consequence is that $\lambda_{1,\text{inter}}$ remains almost constant in the range of few nanometer interdot separations, as shown in Fig. 3(b). Moreover, two s state-like functions are strongly overlapped at smaller d and the anisotropic shape of $\psi_1(r_e, r_h = r_e)$ in individual dots is largely changed. That is why $\lambda_{1,\text{intra}}$ is greatly varied in the strong coupling region. $\psi_4(r_e, r_e)$ is more complicated and there are two nodes along the x axis. It almost disappears at larger d and is largely enhanced at smaller d . The second and third states are always optically inactive. $\psi_2(r_e, r_h = r_e)$, as shown in Fig. 4(c) for an example, is completely antisymmetric.

The Coulomb correlation between the electron and hole is important for InGaAs QDs with sizes that are comparable to or much larger than the exciton Bohr radius. The exciton envelop function will be greatly changed by the Coulomb correlation and thus the exciton fine-structure splitting could be largely influenced. Fine-structure splitting of the exciton ground state in a single QD ($a_0 = 16$ nm, $b_0 = 20$ nm) without the Coulomb cor-

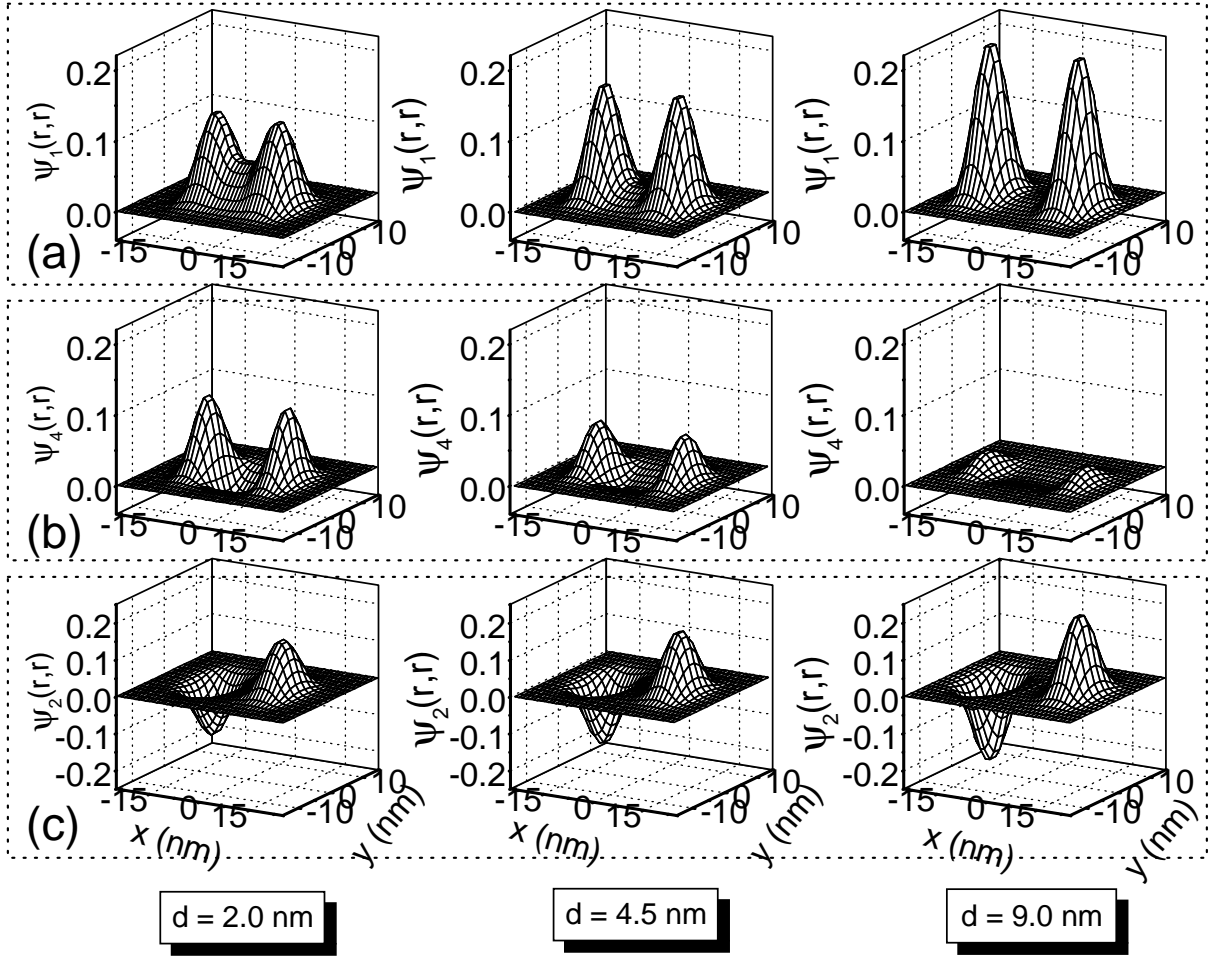


FIG. 4: (a) $\psi_1(r_e, r_h = r_e)$, (b) $\psi_4(r_e, r_h = r_e)$, and (c) $\psi_2(r_e, r_h = r_e)$ of QDM in Fig. 1 for $d = 2.0, 4.5,$ and 9.0 nm, respectively.

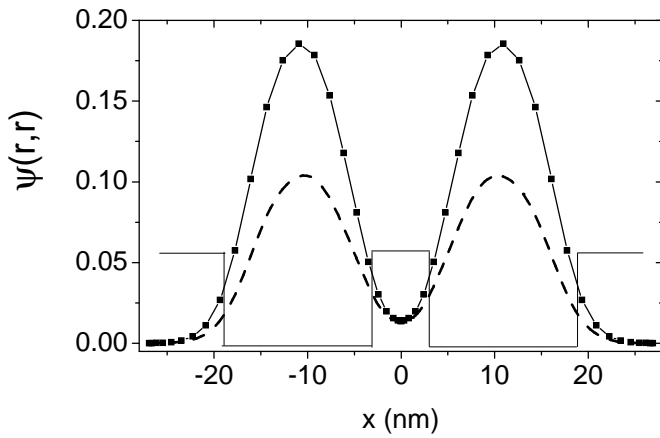


FIG. 5: $\psi(r_e, r_h = r_e)$ along the $y = 0$ axis for the exciton ground state in QDM of Fig. 1 at $d = 6.0$ nm, with (square) and without (dash line) the Coulomb interaction.

relation is $-39 \mu\text{eV}$, the deviation of which from that including the Coulomb correlation is as large as 41%. In QDMs, the Coulomb correlation is also very important. Fine-structure splitting of the exciton ground state without the Coulomb correlation in the same QDM is compared with that taking into account the Coulomb correlation in Fig. 3. It can be seen that the exciton fine-structure splitting is much different between those with and without the Coulomb correlation. For instance, at $d = 6.0$ nm, $\delta_1 \approx 0$ for the case of independent electron and hole, while $\delta_1 = -21 \mu\text{eV}$ for the case of correlated electron and hole. $\psi_1(r_e, r_h = r_e)$ with and without the Coulomb correlation is shown along the $y = 0$ axis in Fig. 5 for $d = 6.0$ nm, respectively. $\psi_1(r_e, r_h = r_e)$ in the correlated case is obviously larger than that in the independent one. That is why the exchange interaction and δ_1 are largely changed by the Coulomb correlation in QDMs.

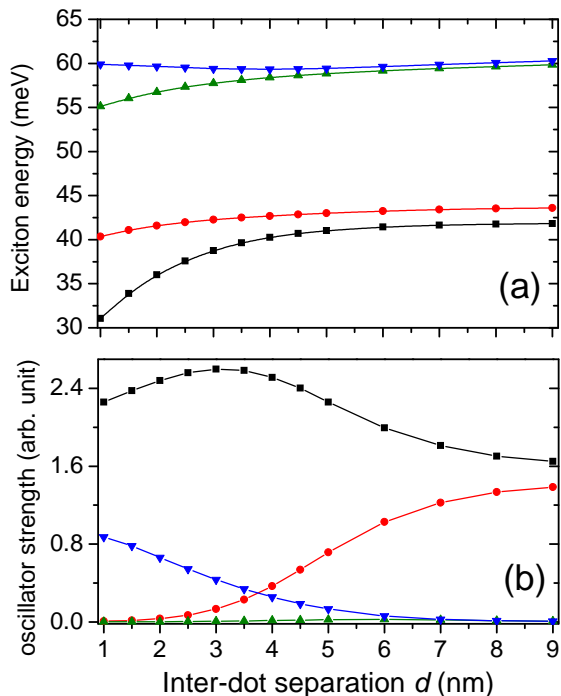


FIG. 6: (Color online) (a) The four-lowest exciton levels without the exchange interaction and (b) the corresponding oscillator strengths as functions of d for two coupled nonidentical dots with $a_0 = a_1 = 16$ nm, $b_0 = 19$ nm, and $b_1 = 20$ nm.

B. Nonsymmetric Quantum Dot Molecule

In experimental growth condition, there is size fluctuation in self-assembled quantum dots and it may be difficult to obtain two coupled identical dots. Thus it is important to study the fine-structure splitting in nonsymmetric QDMs. In Fig. 6(a), the four lowest exciton levels without the exchange interaction for two coupled nonidentical dots with $a_0 = a_1 = 16$ nm, $b_0 = 19$ nm, and $b_1 = 20$ nm are shown as functions of the interdot separation d . As $d > 8.0$ nm, the energies of the exciton ground and second states are much close to the exciton ground state energies of the isolated first and zeroth QDs, respectively. As the separation d decreases, the ground state energy becomes lower. Their oscillator strengths are shown as functions of d in Fig. 6(b). The oscillator strength of the ground state first increases and then decreases while that of the fourth state increases monotonically as d decreases. The third state remains almost optically inactive, and the fourth state becomes optically inactive as $d > 6.0$ nm. In contrast to the identical case as shown in Fig. 2(a), the second level is optically active at larger d and becomes optically inactive as $d < 2.0$ nm.

Fine-structure splittings of three low-lying bright exciton levels are shown as functions of d for the two nonidentical dots in Fig. 7. Similar to the case of two identical dots, δ_1 at larger d is negative, e.g., $\delta_1 = -56$ μeV at

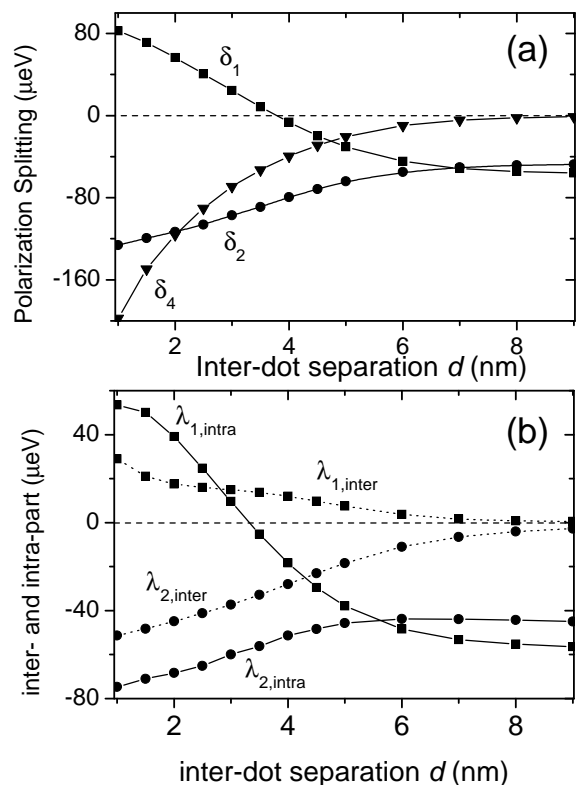


FIG. 7: (a) Fine-structure splitting of the ground (square), second (circle) and fourth (triangle) states of QDM in Fig. 6; (b) $\lambda_{1,\text{intra}}$, $\lambda_{1,\text{inter}}$, $\lambda_{2,\text{intra}}$, and $\lambda_{2,\text{inter}}$ as functions of d .

$d = 9.0$ nm. As d decreases, δ_1 increases monotonically from negative values to positive values. At $d \approx 3.8$ nm, δ_1 is zero. δ_4 decreases from zero at larger d to -150 μeV at $d = 1.5$ nm. The fine-structure splitting δ_2 of ψ_2 decreases from -48 μeV at $d = 9.0$ nm to -97 μeV at $d = 3.0$ nm. Similar to the definition in Eq. 13, the inter- and intradot part of δ_2 can also be given. Fig. 7(b) shows $\lambda_{1(2),\text{inter}}$ and $\lambda_{1(2),\text{intra}}$ as functions of d . $\lambda_{1,\text{intra}}$ is greatly changed from -56 μeV at $d = 9.0$ nm to 54 μeV at $d = 1.0$ nm. In contrast to the identical case, $\lambda_{1,\text{inter}}$ is zero at $d = 9.0$ nm and is increased as d is reduced. For ψ_2 , $\lambda_{2,\text{inter}}$ ($\lambda_{2,\text{intra}}$) is decreased from -3 μeV (-45 μeV) at $d = 9.0$ nm to -37 μeV (-60 μeV) at $d = 3.0$ nm.

In nonidentical cases, $\psi_1(r_e, r_h = r_e)$ is almost localized in the larger dot at $d = 9.0$ nm as shown in Fig. 8(a) and therefore $\lambda_{1,\text{inter}}$ becomes zero at larger d as shown in Fig. 7(b). Similar to the identical case, $\psi_4(r_e, r_e)$ has two nodes along the x axis and almost vanishes at larger d . $\psi_2(r_e, r_e)$ is much localized in the smaller dot at $d = 9.0$ nm as shown in Fig. 8(c) and therefore $\lambda_{2,\text{inter}}$, similar to $\lambda_{1,\text{inter}}$, also becomes zero at larger d . Since the symmetries of $\psi_1(r_e, r_e)$ and $\psi_2(r_e, r_e)$ are opposite, $\lambda_{1,\text{inter}}$ and $\lambda_{2,\text{inter}}$ have opposite signs, i.e., $\lambda_{1,\text{inter}} > 0$ and $\lambda_{2,\text{inter}} < 0$.

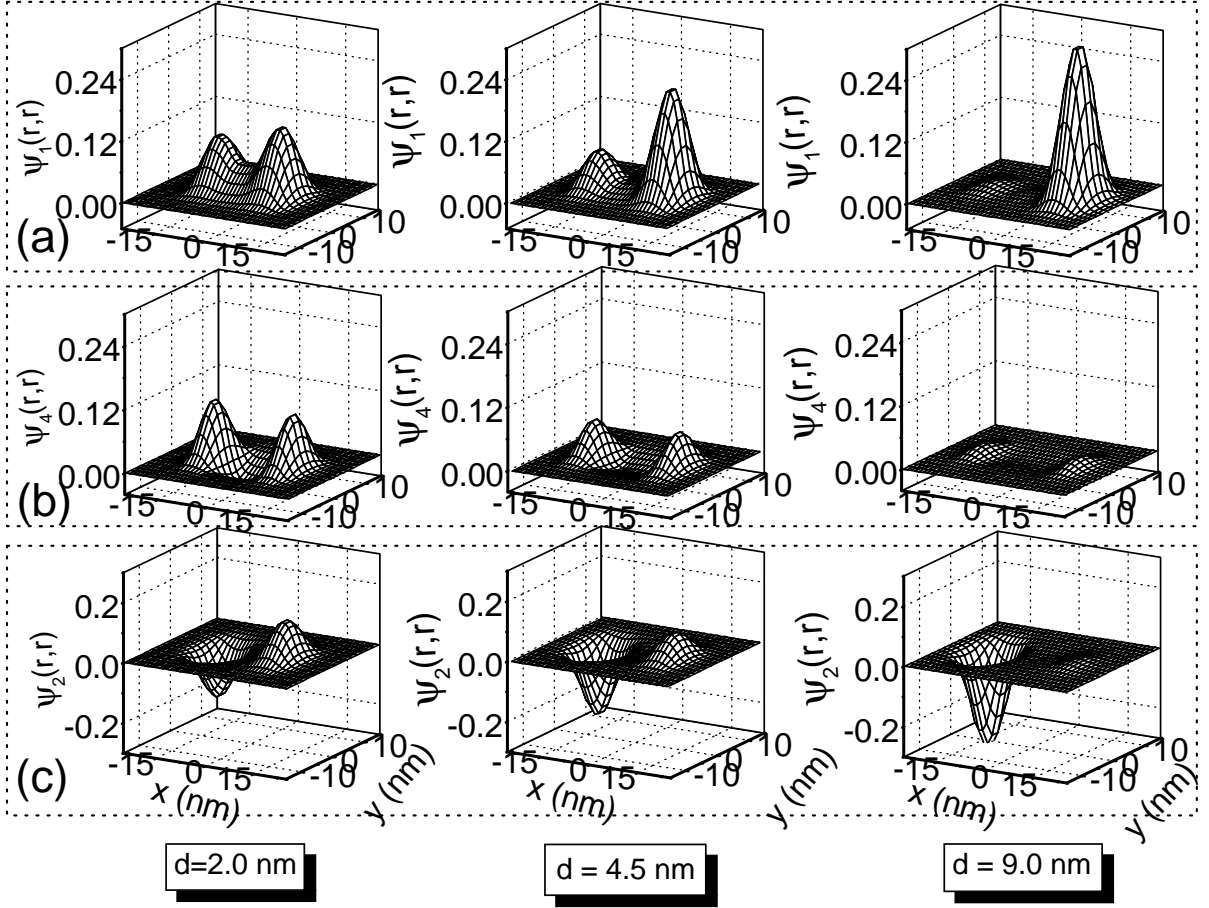


FIG. 8: (a) $\psi_1(r_e, r_h = r_e)$, (b) $\psi_4(r_e, r_h = r_e)$, and (c) $\psi_2(r_e, r_h = r_e)$ of QDM in Fig. 6 for $d = 2.0, 4.5,$ and 9.0 nm, respectively.

IV. SUMMARY

We formulate a microscopic theory of exciton fine-structure splitting in laterally-coupled QDM taking into account the Coulomb correlation between the electron and hole. We choose the sizes of QDs resembling those grown in experiments. In typical QDM, the electron and hole tunneling energies and the direct Coulomb interaction are essential for the exciton levels and envelop functions. As the inter-dot separation is reduced, fine-structure splitting of the exciton ground state in QDM is largely increased while those of the second and fourth states are decreased. At a proper separation, fine-structure splitting of the ground state approaches zero. Fine-structure splittings of the exciton ground and first-excited states could be divided into the intra- and interdot exchange interactions, which are sensitive to the tunnel-coupling and symmetry of QDMs. In symmetric QDMs, the inter-dot part is almost unchanged in the range of few nanometer interdot separation, while in non-

symmetric QDMs the inter-dot part is rapidly reduced to zero at larger inter-dot separation. In both symmetric and nonsymmetric cases, the intra-dot part is greatly varied by the tunnel-coupling, and the fine-structure splitting of the exciton ground state could be varied by about hundred μeV . The fine-structure splitting of the fourth state is greatly enhanced at smaller d while approaches zero at larger d . In summary, the study provides an efficient way of largely tuning the exciton fine-structure splitting in semiconductor QDs, which is useful and necessary for the fine-tuning by the external field.

Acknowledgments

Financial supports from NSF-China (Grant No. 10574077), the “863” Programme (No. 2006AA03Z0404) and MOST Programme (No. 2006CB0L0601) of China are gratefully acknowledged.

- * Electronic address: zjl-dmp@tsinghua.edu.cn
- ¹ P. Michler, A. Imamoglu, M.D. Mason, P.J. Carson, G.F. Strouse, and S.K. Buratto, *Nature (London)*, **406**, 968 (2000).
 - ² P. Michler, A. Kiraz, C. Becher, W.V. Schoenfeld, P.M. Petroff, L.D. Zhang, E. Hu, and A. Imamoglu, *Science*, **290**, 2282 (2000).
 - ³ C. Santori, D. Fattal, J. Vučković, G.S. Solomon, and Y. Yamamoto, *Nature (London)*, **419**, 594 (2002).
 - ⁴ M. Pelton, C. Santori, J. Vučković, B.Y. Zhang, G.S. Solomon, J. Plant, and Y. Yamamoto, *Phys. Rev. Lett.* **89**, 233602 (2002).
 - ⁵ C. Santori, D. Fattal, M. Pelton, G.S. Solomon, and Y. Yamamoto, *Phys. Rev. B* **66**, 045308 (2002).
 - ⁶ R.M. Stevenson, R.J. Young, P. Atkinson, K. Cooper, D.A. Ritchie, and A.J. Shields, *Nature (London)*, **439**, 179 (2006).
 - ⁷ N. Akopian, N.H. Lindner, E. Poem, Y. Berlatzky, J. Avron, D. Gershoni, B.D. Gerardot, and P.M. Petroff, *Phys. Rev. Lett.* **96**, 130501 (2006).
 - ⁸ O. Benson, C. Santori, M. Pelton, and Y. Yamamoto, *Phys. Rev. Lett.* **84**, 2513 (2000).
 - ⁹ D. Gammon, E.S. Snow, B.V. Shanabrook, D.S. Katzer, and D. Park, *Phys. Rev. Lett.* **76**, 3005 (1996).
 - ¹⁰ M. Bayer, A. Kuther, A. Forchel, A. Gorbunov, V.B. Timofeev, F. Schäfer, J.P. Reithmaier, T.L. Reinecke, and S.N. Walck, *Phys. Rev. Lett.* **82**, 1748 (1999).
 - ¹¹ R. Seguin, A. Schliwa, S. Rodt, K. Potschke, U.W. Pohl, and D. Bimberg, *Phys. Rev. Lett.* **95**, 257402 (2005).
 - ¹² E.L. Ivchenko, *Phys. Status Solidi A* **164**, 487 (1997).
 - ¹³ T. Takagahara, *Phys. Rev. B* **62**, 16840 (2000).
 - ¹⁴ G. Bester, Selvakumar Nair, and A. Zunger, *Phys. Rev. B* **67**, 161306(R) (2003).
 - ¹⁵ A.I. Tartakovskii, M.N. Makhonin, I.R. Sellers, J. Cahill, A.D. Andreev, D.M. Whittaker, J-P.R. Wells, A.M. Fox, D.J. Mowbray, M.S. Skolnick, K.M. Groom, M.J. Steer, H.Y. Liu, and M. Hopkinson, *Phys. Rev. B* **70**, 193303 (2004).
 - ¹⁶ W. Langbein, P. Borri, U. Woggon, V. Stavarache, D. Reuter, and A.D. Wieck, *Phys. Rev. B* **69**, 161301(R) (2004).
 - ¹⁷ R.J. Young, R.M. Stevenson, A.J. Shields, P. Atkinson, K. Cooper, D.A. Ritchie, K.M. Groom, A.I. Tartakovskii, and M.S. Skolnick, *Phys. Rev. B* **72** 113305 (2005).
 - ¹⁸ A. Greilich, M. Schwab, T. Berstermann, T. Auer, R. Oulton, D.R. Yakovlev, M. Bayer, V. Stavarache, D. Reuter, and A. Wieck, *Phys. Rev. B* **73**, 045323 (2006).
 - ¹⁹ R.M. Stevenson, R.J. Young, P. See, D.G. Gevaux, K. Cooper, P. Atkinson, I. Farrer, D.A. Ritchie, and A.J. Shields, *Phys. Rev. B* **73**, 033306 (2006).
 - ²⁰ K. Kowalik, O. Krebs, A. Lemaitre, S. Laurent, P. Senellart, P. Voisin, J.A. Gaj, *Appl. Phys. Lett.* **86**, 041907 (2005).
 - ²¹ B.D. Gerardot, S. Seidl, P.A. Dalgarno, R.J. Warburton, D. Granados, J.M. Garcia, K. Kowalik, O. Krebs, K. Karrai, A. Badolato, and P.M. Petroff, *Appl. Phys. Lett.* **90**, 041101 (2007).
 - ²² M. Bayer, O. Stern, A. Kuther, and A. Forchel, *Phys. Rev. B* **61**, 7273 (2000).
 - ²³ M. Bayer, G. Ortner, O. Stern, A. Kuther, A.A. Gorbunov, A. Forchel, P. Hawrylak, S. Fafard, K. Hinzer, T.L. Reinecke, S.N. Walck, J.P. Reithmaier, F. Klopff, and F. Schafer, *Phys. Rev. B* **65**, 195315 (2002).
 - ²⁴ M. Bayer, P. Hawrylak, K. Hinzer, S. Fafard, M. Korkusinski, Z.R. Wasilewski, O. Stern, and A. Forchel, *Science*, **291**, 451 (2001).
 - ²⁵ G. Ortner, I. Yugova, G.B.H. von Högersthal, A. Larionov, H. Kurtze, D.R. Yakovlev, M. Bayer, S. Fafard, Z. Wasilewski, P. Hawrylak, Y.B. Lyanda-Geller, T.L. Reinecke, A. Babinski, M. Potemski, V.B. Timofeev, and A. Forchel, *Phys. Rev. B* **71**, 125335 (2005).
 - ²⁶ B.D. Gerardot, S. Strauf, M.J.A. de Dood, A.M. Bychkov, A. Badolato, K. Hennessy, E.L. Hu, D. Bouwmeester, and P.M. Petroff, *Phys. Rev. Lett.* **95**, 137403 (2005).
 - ²⁷ T. Unold, K. Mueller, C. Lienau, T. Elsaesser, and A.D. Wieck, *Phys. Rev. Lett.* **94**, 137404 (2005).
 - ²⁸ G.J. Beirne, C. Hermannstädter, L. Wang, A. Rastelli, O.G. Schmidt, and P. Michler, *Phys. Rev. Lett.* **96**, 137401 (2006).
 - ²⁹ G. Ortner, M. Bayer, A. Larionov, V.B. Timofeev, A. Forchel, Y.B. Lyanda-Geller, T.L. Reinecke, P. Hawrylak, S. Fafard, and Z. Wasilewski, *Phys. Rev. Lett.* **90**, 086404 (2003).
 - ³⁰ G. Ortner, M. Bayer, Y. Lyanda-Geller, T.L. Reinecke, A. Kress, J.P. Reithmaier, and A. Forchel, *Phys. Rev. Lett.* **94**, 157401 (2005).
 - ³¹ H.J. Krenner, M. Sabathil, E.C. Clark, A. Kress, D. Schuh, M. Bichler, G. Abstreiter, and J.J. Finley, *Phys. Rev. Lett.* **94**, 057402 (2005).
 - ³² B. Szafran, F.M. Peeters, and S. Bednarek, *Phys. Rev. B* **75**, 115303(2007).
 - ³³ B. Szafran, T. Chwiej, F.M. Peeters, S. Bednarek, J. Adamowski, and B. Partoens, *Phys. Rev. B* **71**, 205316(2005).
 - ³⁴ G. Bester, and A. Zunger, *Phys. Rev. B* **72**, 165334(2005).
 - ³⁵ J.L. Zhu, W. Chu, D. Xu, and Z. Dai, *Appl. Phys. Lett.* **87**, 263113(2005).
 - ³⁶ G. Bester, A. Zunger, and J. Shumway, *Phys. Rev. B* **71**, 075325 (2005).
 - ³⁷ J.L. Zhu, and D. Xu, cond-mat/07043871 (to appear in *Appl. Phys. Lett.*).
 - ³⁸ W.D. Sheng, and P. Hawrylak, *Phys. Rev. B* **73**, 125331 (2006).
 - ³⁹ R. Ugajin, T. Suzuki, K. Nomoto, and I. Hase, *J. Appl. Phys.* **76**, 1041 (1994).
 - ⁴⁰ A. Nazir, B.W. Lovett, S.D. Barrett, J.H. Reina, and G.A.D. Briggs, *Phys. Rev. B* **71**, 045334 (2005).